Paleomagnetic dating of a mysterious lake record from the Kerguelen archipelago by matching to paleomagnetic field models

Kim Teilmann

Dissertations in Geology at Lund University,
Bachelor's thesis, no. 480
(15 hp/ECTS credits)

Department of Geology
Lund University
2016

Paleomagnetic dating of a mysterious lake record from the Kerguelen archipelago by matching to paleomagnetic field models

Bachelor's thesis

Kim Teilmann

Department of Geology
Lund University
2016

Contents

Cover Picture: Lake Cocytus. Photo by Nathalie Van der Putten.

Paleomagnetic dating of a mysterious lake record from the Kerguelen archipelago by matching to paleomagnetic field models

KIM TEILMANN

Teilmann, K., 2016: Paleomagnetic dating of a mysterious lake record from the Kerguelen archipelago by matching to paleomagnetic field models. *Dissertations in Geology at Lund University*, No. 480, 22 pp. 15 hp (15 ECTS credits).

Abstract: The Kerguelen archipelago is a volcanic island group in the southern Indian Ocean. It is located on the polar front as well as within the Circumpolar Antarctic Current and the Southern Hemisphere Westerly Wind Belt. This makes it an interesting location for paleoclimate studies. For this reason, a three meter long sediment sequence from a lake on the archipelago was retrieved in 2013. Radiocarbon dating of the lake record revealed a puzzling result with the occurrence of several age reversals. This study aims at improving the understanding of the chronology of the sequence by establishing an age-depth model based on comparison of the characteristic remanent magnetization of the sediment with the *pfm9k.1a* and *A_FM* paleomagnetic models.

Alternating field demagnetization up to 80 mT applied to 153 discrete samples revealed the presence of a viscous component that was removed after demagnetization steps of 10 to 15 mT. Investigation of the sediment stratigraphy and the characteristic remanent magnetization indicates that part of the lake sequence consists of slump deposits. The declination and inclination of the sediment presumed to be in situ shows similarities with the *A_FM* model, and a simple age-depth model for the lower half of the sequence has been constructed by correlation of inclination and declination features.

The established age-depth model shows discrepancies of up to a couple of hundred years when compared with the radiocarbon dates. The discrepancies might be explained by limitations of the paleomagnetic models, as these are mainly based on paleomagnetic data from the northern hemisphere, but difficulties in the interpretation of the sediment stratigraphy might play a role as well. Radiocarbon dating of samples from a few identified key horizons is suggested to improve the understanding of the chronology of the sediment sequence.

Keywords: Paleomagnetism, paleomagnetic field models, paleomagnetic secular variation, Kerguelen archipelago, lake sediment, slump deposits

Supervisors: Andreas Nilsson & Nathalie Van der Putten

Subject: Quaternary Geology

Kim Teilmann, Department of Geology, Lund University, Sölvegatan 12, SE-223 62 Lund, Sweden. E-mail: nat13kte@student.lu.se

Paleomagnetisk datering av ett mystiskt sjösediment från Kerguelenöarna vid jämförsel med paleomagnetiska fältmodeller

KIM TEILMANN

Teilmann, K., 2016: Paleomagnetisk datering av ett mystiskt sjösediment från Kerguelenöarna vid jämförsel med paleomagnetiska fältmodeller. *Examensarbeten i geologi vid Lunds universitet*, Nr. 480, 22 sid. 15 hp.

Sammanfattning: Kerguelenöarna är en vulkanisk ögrupp belägen i det södra Indiska oceanen. Öarna ligger på polarfronten samt inom den cirkumpolära Antarktiska strömmen och södra halvklotets västvindsbälte. Detta gör Kerguelenöarna till en intressant plats för klimatstudier. Av denna anledning erhölls en tre meter lång sekvens av sediment från en sjö på ögruppen 2013. Kol-14 datering av sjösedimenten gav ett gåtfullt resultat med förekomst av flera åldersomkastningar. Denna studie syftar till att förbättra förståelsen av sedimentens kronologi genom att skapa en ålders-djup-modell baserad på jämförelse av sedimentens karakteristiska remanenta magnetisering med de paleomagnetiska modellerna *pfm9k.1a* och *A_FM*.

Avmagnetisering av 153 prover med alternerande fält upp till 80 mT avslöjade en viskös komponent som avlägsnades efter avmagnetiseringssteg på 10 till 15 mT. Undersökning av sedimentstratigrafin och den karaktäristiska remanenta magnetiseringen tyder på att delar av sekvensen har avsatts i samband med massflöden. Deklinationen och inklinationen i de sedimenten som antas vara in situ uppvisar likheter med *A_FM*, och en simpel ålders-djup-modell för den nedre halvan av sekvensen har konstruerats genom korrelation av utmärkande deklinations- och inklinationshändelser.

Den etablerade ålders-djup-modellen visar skillnader på upp till ett par hundra år jämfört med kol-14 dateringarna. Avvikelserna kan möjligvis förklaras av begränsningar av de paleomagnetiska modellerna, eftersom dessa huvudsakligen är baserade på paleomagnetisk data från norra halvklotet, men svårigheter vid tolkningen av sedimentetstratigrafin kan också vara en medverkande faktor. Ytterligare kol-14-dateringar av strategiskt utvalda delar av sedimentsekvensen rekommenderad för att förbättra förståelsen av kronologin.

Nyckelord: Paleomagnetism, paleomagnetiska fältmodeller, paleomagnetiska sekulära variationer, Kerguelenöarna, sjösediment, massflöden

Handledare: Andreas Nilsson & Nathalie Van der Putten

Ämnesinriktning: Kvartärgeologi

Kim Teilmann, Geologiska institutionen, Lunds universitet, Sölvegatan 12, 223 62 Lund, Sverige. E-post: nat13kte@student.lu.se

1 Introduction

Studying past climate variability is of great importance for understanding the mechanisms of ongoing global climate change. Historical records can give some insight, but are limited in space and time. In order to study historically unrecorded climate variations, it is therefore necessary to acquire and study naturally preserved climate proxies. Climate proxies, such as diatom assemblages and oxygen isotopes measured in sediments have successfully been used to reconstruct variations in local and global ice volumes and temperatures (e.g. Lisiecki & Raymo 2005; Fernandez et al. 2013).

In December of 2013, three sequences of lake sediments, consisting of four to five cores each, were retrieved from the Kerguelen archipelago, remotely located in the South Indian Ocean. Few terrestrial paleoclimate records from this area exist, so the lake sediments may provide new insights to the climate history of the area. In addition, paleoclimate data from the Kerguelen archipelago might contribute to a better understanding of past changes in oceanic and atmospheric circulation due to its location at the Polar Front within the Circumpolar Antarctic Current and the Southern Hemisphere Westerly Wind Belt (Van der Putten et al. 2015).

In order to compare and correlate the paleoclimate data found within the lake sediments with existing records, establishing a chronology for the sequences is essential. An attempt to establish a chronology has been made based on radiocarbon dating of plant macrofossils and bulk samples. The samples yielded ages between present day and 2230 uncalibrated ^{14}C years BP (before present), but with the occurrence of several yet unexplainable reversals. Application of an alternative dating method can be helpful to the interpretation of the enigmatic radiocarbon dates.

One alternative dating method is the use of past variations of the geomagnetic field, recorded by magnetic minerals contained within the lake sediments. An age-depth model of the sediment sequences can be obtained by comparing their paleomagnetic data with that of an independently dated record from a nearby location or with modelled paleomagnetic field predictions, a method successfully applied to Arctic marine sediments by Barletta et a. (2010).

This study aims to establish an age-depth model for the Kerguelen lake sequences based on the remanent magnetization of the sediment. Preliminary measurements have shown that the lake record carry a strong and stable magnetization. Unfortunately, there are no available independently dated paleomagnetic records within the upper practical limit for Holocene paleomagnetic pattern matching, estimated to be around 2000 km by Thompson & Oldfield (1982). Instead, a potential age-depth model will be established by comparison with field predictions according to paleomagnetic field models *pfm9k.1a* by Nilsson et al. (2014) and *A_FM* by Licht et al. (2013).

2 Study area

The Kerguelen archipelago is a French territory comprising more than 300 islands. The total area of the archipelago is 6500 km² (Damasceno et al. 2002), of which the main island covers 6000 km² (Hall 1984). It is located in the Southern Indian Ocean between latitudes 48° to 50° south (Fig. 1A) as part of Terres Australes et Antarctiques Francaises (French Southern and Antarctic Lands).

The archipelago is part the Kerguelen Plateau, a Large Igneous Province that rises more than 2000 meters above the surrounding ocean basins (Benard et al. 2010). The bedrock consists mainly of flood basalts of ages between 24 and 29 million years, with the occurrence of several plutonic complexes throughout the area and of Quaternary deposits in the eastern parts (Damasceno et al. 2002).

As of 2001, the total ice cover amounted to about 500 km² with the biggest contribution from the Cook ice cap covering about 410 *km²* (Cogley et al. 2014), but it is likely that ice covered the entire main island during the last glacial period (Hall 1984). Evidence of widespread ice cover is prevalent, as the archipelagos topography is characterized by the presence of numerous valleys and fjords produced by glacial erosion (Damasceno et al. 2002).

The sediment sequences were retrieved from an unnamed lake, possibly a tarn, on the south eastern lower flank of Mount Carbenay in the central southern area Plaine de Dante (Fig. 1B-C). I suggest the name Lake Cocytus[1], and will refer to it as such from this point on. The lake is sub-circular with a maximum shore-to-shore length of 240 meters. Shallow areas of widths between a few and 60 meters extend from the lake shore. From the edge of the shallow areas, the lake floor slopes steeply to a maximum depth of approximately ten meters (Fig. 1D). The catchment area is restricted to the slopes of the immediate surroundings.

[1]Lake Cocytus is mentioned by Dante in his Divine Comedy. Since the lake is located in Plaine de Dante, I considered this an appropriate name.

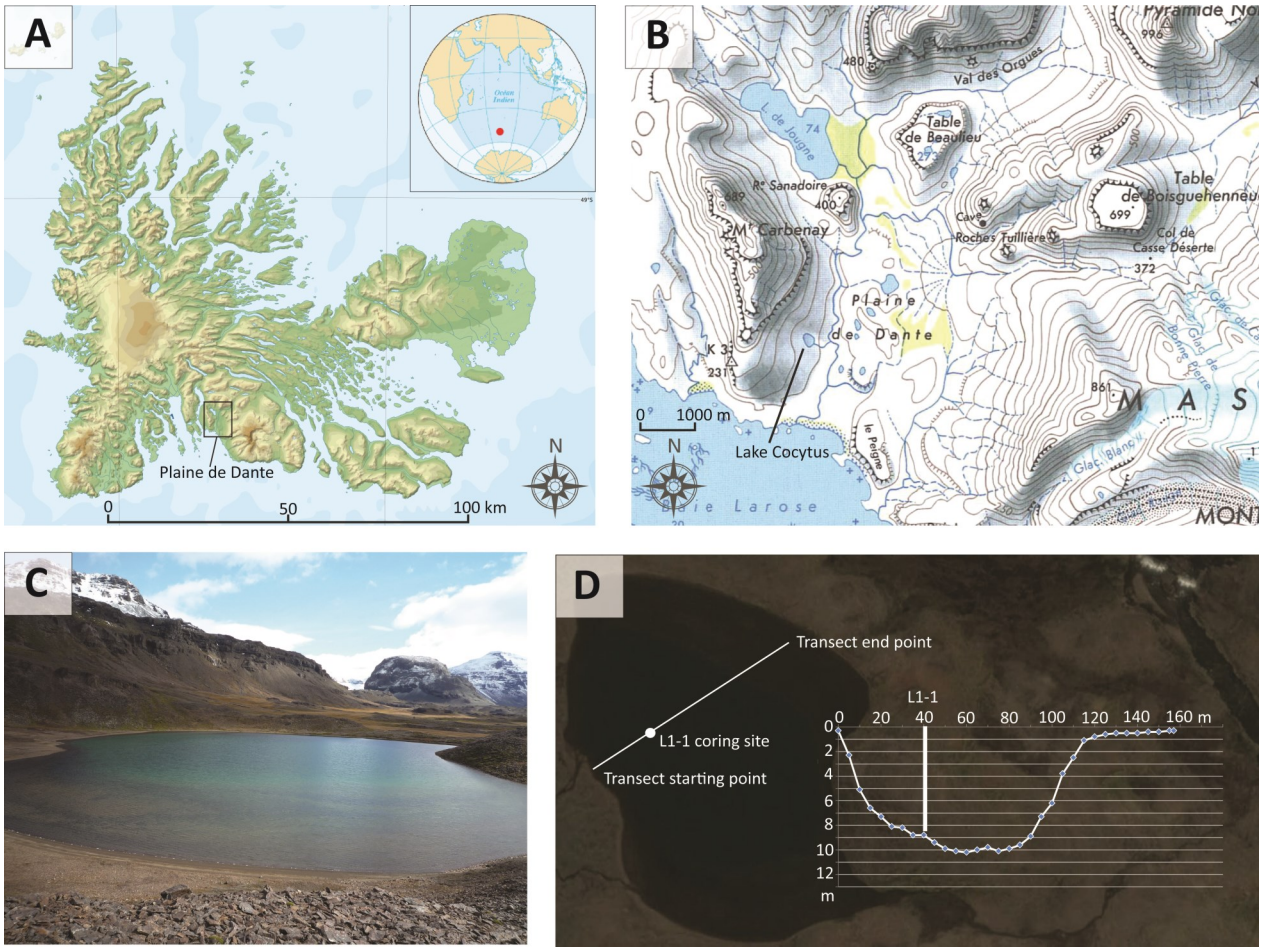

Fig. 1. **A**. Map showing the location of the study area and the Kerguelen archipelago. Adapted from map by Rémi Kaupp at Wiki Commons. **B**. Map of the study area showing the location of Lake Cocytus. Adapted from atlas scan downloaded from the French government's geoportail website (www.geoportail.gouv.fr). **C**. Picture of Lake Cocytus with a northerly view. Picture by Nathalie Van der Putten. **D**. Transect of Lake Cocytus with location of coring site for sediment sequence L1-1. Background image from Google Earth.

3 Theoretical background

A basic understanding of the principals involved in the acquisition of a remanent magnetization is important in order to understand the dating method. A basic description of the underlying principles is provided in this section. For more detailed descriptions, the interested reader is referred to textbooks on the subject (Thompson & Oldfield 1982; Butler 1992).

3.1 Magnetic terms

A magnet consists of a magnetic dipole with two magnetic poles of opposite polarity. The product of the size of the magnetic charges and the distance between them is termed the magnetic moment (SI-unit: Am^2), and is a vector pointing in direction from the negative to the positive pole (Butler 1992). Any magnetic dipole is surrounded by magnetic field lines that flow from pole to pole in a radial pattern, and if a magnetic unit is placed within the field, it encounters what is called a magnetic field force (SI-unit: Am^{-1}) (Butler 1992), that either attracts or repels it depending on polarity.

A material may contain several individual magnetic dipoles of varying orientation. The term magnetization (SI-unit: T) is of great importance, and refers to the net magnetic moment per unit volume of a material. Depending on composition, a material that is within the range of an external magnetic field may develop an induced magnetization (Butler 1992) caused by interactions between the external field and the magnetic dipoles present in the material. The size of the induced magnetization depends on the magnetic susceptibility (SI-unit: dimensionless if volume specific) of the material and the strength of the magnetic field force. In some materials, a remanent magnetization caused by past magnetic fields may be present as will be discussed in section 3.3.

3.2 The geomagnetic field

Earth is surrounded by a magnetic field, originating from flow within the liquid outer core of the planet (Butler 1992). This flow generates a geomagnetic field that to approximately 90% can be explained by a dipole placed at the centre of Earth, slightly inclined to Earth's rotational axis. The poles of the geomagnetic dipole are referred to as the magnetic north and south poles (Fig. 2).

Averaged over sufficient time, the geomagnetic dipole coincides with Earth's rotational axis, a phenomenon conceptually known as the geocentric axial dipole (GAD).

The actual geomagnetic dipole is dynamic and moves relative to the geographical poles. The location of the magnetic poles at any given time can be described by the two location-dependent properties declination and inclination (Fig. 3).

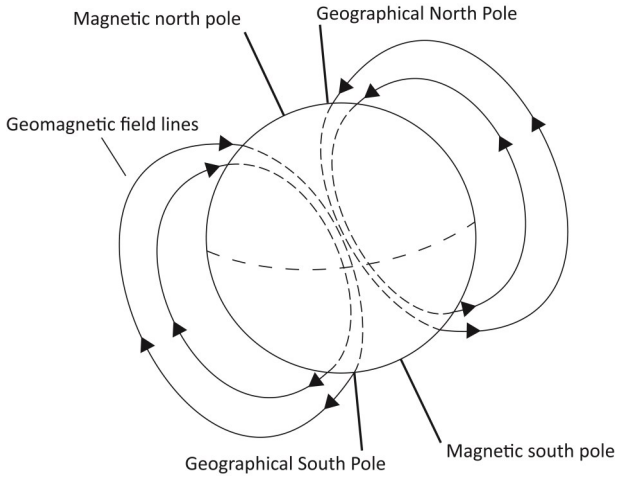

Fig. 2. Sketch of the dipole part of Earth's magnetic field. Note the inclination of the dipole to Earth's rotational axis and the radial pattern of the magnetic field lines flowing from the magnetic south pole to the magnetic north pole. Adapted from sketch by TStein at Wiki Commons.

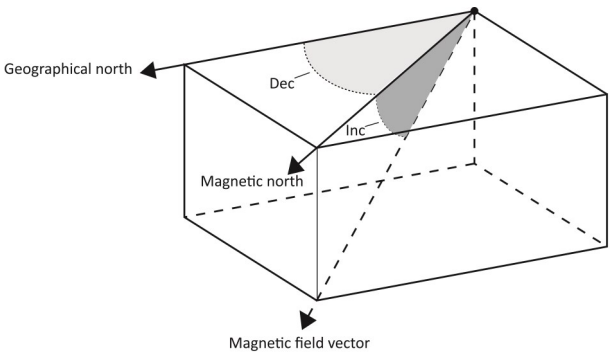

Fig. 3. Sketch illustrating the concepts of magnetic declination (Dec) and inclination (Inc). Declination is the angle between magnetic north and geographical north measured at a given location. Inclination is the angle between a magnetic field line and horizontal.

Declination refers to the angle between the geographic and the magnetic north pole, while inclination is the angle between the magnetic field lines and the horizon (Thompson & Oldfield 1982). Declinations towards west are reported as negative values, while easterly declinations are reported as positive. For inclination values, a downward dip of the north-seeking end of a dipole below the horizon is reported as positive, while an upwards dip is reported as negative (Thompson & Oldfield 1982).

3.2.1 Paleomagnetic secular variation

As mentioned in the previous section, the orientation of the geomagnetic field varies over time. These variations can be categorized based on their magnitude and periodicity. Paleomagnetic secular variations are changes that occur over a timespan of one to 10.000 years that can be recognized over sub-continental regions (Butler 1992). The main cause of secular variations is flow-variation in the outer core (Constable & Constable 2004) with contributions from both the dipole and the so-called non-dipole fields (Butler 1992). Records of past variations can be found in the natural remanent magnetization of appropriate geological materials.

3.3 Natural remanent magnetization

A magnetization caused by past magnetic fields that has been preserved in a material by natural processes is called a natural remanent magnetization (NRM). A NRM usually consists of a primary and a secondary component. Primary components are acquired during rock formation or sediment deposition, while secondary components are acquired later (Butler 1992). Depending on the mineral assemblage, a remanent magnetization may decay over time, in a process known as magnetic relaxation. NRM can result from several processes, but the processes of greatest interest to this study are those that govern the acquisition of detrital remanent magnetization and viscous remanent magnetization.

3.3.1 Depositional remanent magnetization

Detrital material (e.g. lake sediment) can carry a depositional remanent magnetization (DRM) if magnetic minerals are present. As sediment settles in low energy environments, a fraction of the magnetic minerals are aligned with the prevailing geomagnetic field at the time of deposition. According to Butler (1992), the alignment may continue post-depositionally in the uppermost ten to twenty cm of the accumulating sediment. When further movement of the sediment particles is no longer possible due to dewatering and con-

solidation, the DRM is locked-in (Butler 1992), preserving a record of the geomagnetic field from deposition to lock-in.

3.3.2 Viscous remanent magnetization

Viscous remanent magnetization (VRM) is acquired over time after lock-in of DRM. Whereas DRM is a physical process of mineral alignment, VRM is produced by changes within magnetic minerals with relatively short magnetic relaxation times. In a slow process, these minerals continuously change their magnetization to align with the ambient magnetic field (Butler 1992). The processes behind these changes are too complex to describe for the purpose of this study, but it is important to know that some magnetic grains are more susceptible to viscous magnetization than others.

Zijderveld (1967) refers to the smallest strength of the magnetic field required to change the direction of a magnetization as its release force. In the presence of a weak magnetic field, such as Earth's, only magnetic moments with low release forces (short relaxation times) develop a VRM. This implies that some of the magnetic grains in a sediment sample may remain practically unaffected by the geomagnetic field after lock-in of the DRM.

VRM does not provide information about the geomagnetic field at the time of deposition, and is commonly eliminated in the laboratory by exposure to alternating field demagnetization.

3.4 Progressive AF demagnetization

The method of progressive alternating field (AF) demagnetization aims to cancel the VRM by exposure to a series of alternating magnetic field cycles. Each cycle begins with a peak intensity that subsequently decreases while the field direction alternates between two opposites. From one cycle to the next, the peak intensity is increased. With each cycle, the magnetic dipoles with release forces less than that of the peak AF intensity are aligned randomly in opposite directions, effectively cancelling each other out (Butler 1992). By increasing the peak intensity of the AF between cycles, a continuously greater proportion of the NRM is cancelled with each step. At sample-specific peak intensities, all VRM is eliminated, while a stronger magnetization remains.

3.5 Characteristic magnetization

The high stability component of the NRM that remains after the removal of VRM or other secondary magnetizations of low stability is referred to as the characteristic remanent magnetization (ChRM) (Zijderveld 1967; Butler 1992). Under optimal conditions, the remaining high stability component of the NRM corresponds to the DRM, but since other magnetizations may be present as well, ChRM is used to avoid false statements. The parameters being matched to the paleomagnetic models in this study are the declinations and inclinations of the lake record ChRM.

4 Method

4.1 Field work

In December of 2013, field work was carried out by Nathalie Van der Putten (Department of Geology, Lund University), Elisabeth Michel (Climate and Environment Sciences Laboratory, Gif-sur-Yvette, France) and Bart Klinck (volunteer). Three sediment sequences named L1, L2 and L3 were retrieved from Lake Cocytus within 10 meters of each other, using a Russian corer at water depths around nine meters. Each sequence consists of four to five overlapping cores with a total length of around three meters. The cores were collected onboard a boat fixed by lines secured by the lake side. Care was taken to minimize orientation variation between cores.

4.2 Radiocarbon dating

A total of 11 samples were collected from sequence L3 and submitted to the Single Stage AMS at Lund University and the CEA Saclay in France for radiocarbon dating. The samples were collected by Nathalie Van der Putten and consist of three bulk samples, three samples of mosses and five samples of leafs or seeds from the flowering plant *Azorella selago*.

4.3 Sub-sampling for magnetic measurements

The standard method of discrete sampling by pushing sampling cubes into the sediment core, posed a large risk of sediment disturbance due to the presence of mosses in sections of the sequence. Instead, subsamples were precut with knives of stainless steel and low magnetization (to lower the risk of magnetic contamination).

Rectangular blocks of sediment with a cross sectional area of 1.9 x 1.9 cm and a minimum height of 2 cm were cut wall-to-wall along the cores. Where coarseness or lack of cohesion of the sediment prevented preservation of internal fabric, sub-sampling was omitted. Subsequently, paleomagnetic sampling cubes with inner dimensions of 2 x 2 x 2 cm were aligned above the precut rectangles, and pushed down

to enclose the sub-sample. A hole through the cube wall opposite the opening allowed for air escape during the procedure. Sediment protruding from the cube opening was removed using a knife, and a lid was attached. The sub-samples were stored in airtight containers at ~4°C prior to magnetic measurements.

Four cores from sequence L1 were subsampled according to Table 1. The three cores named L1-1, L1-3 and L1-5 were sub-sampled along their entire lengths when possible, while only a shorter section of core L1-4 was sub-sampled. A total of 153 sub-samples were obtained for magnetic measurements.

4.4 Magnetic measurements predating the study

Prior to this study, measurement of the magnetic susceptibility of the cores was carried out by Nathalie Van der Putten using a Barington Instruments Ltd MS2E1 sensor and a TAMISCAN-TS1 conveyer belt.

4.5 Magnetic measurements

AF demagnetization and measurement of the NRM of the sub-samples was carried out using a 2G Enterprises Model 760 cryogenic magnetometer equipped with in-line AF demagnetization coils at the paleomagnetic laboratory at the University of Lund, Sweden. Sub-samples were demagnetized along three orthogonal axes (x, y and z in the Cartesian coordinate system) by exposure to progressive alternating fields with peak intensities of 0, 5, 10, 15, 20, 30, 40, 50, 60, 70 and 80 mT. The magnetization was measured after each step of the demagnetization series. The ChRM was identified with Zijderveld plots and the declination and inclination of the ChRM was determined in MATLAB by the application of the principal component analysis described by Kirschvink (1980) using a free fit.

Due to time limitations, eight sub-samples (Table 2) were chosen for further magnetic measurements comprising anhysteretic remanent magnetization (ARM) and isothermal remanent magnetizations (IRM). The ARM was imparted in the cryogenic magnetometer with an application of an 80 mT alternating field and an underlying direct current bias field of 0.05 mT. The ARM was subsequently demagnetized using the same demagnetization steps as for the NRM, including measurement of magnetization intensity following each step.

After ARM-demagnetization, two IRM's were imparted on the eight samples. To achieve an assumed saturation isothermal remanent magnetization (SIRM), a direct current field of 1T was applied for 1ms using a Redcliffe 700-BSM pulse magnetizer. A field of 300mT in the opposite direction was later applied for 1ms in a Molspin pulse magnetizer. Following each IRM-acquisition, the magnetization intensity of the sub-samples was measured in a Molspin Minispin Magnetometer.

Table 1. Overview of the core sections sub-sampled for magnetic measurements.

Core ID	Core depth (cm)	Section sampled (cm[a])	Total samples
L1-1	0-100	0-98.5	52
L1-3	83-183	2-93.5	46
L1-4	150-250	17-48.6	17
L1-5	219-319	28.5-100	38

[a]Refers to depth within cores

4.6 Paleomagnetic field predictions

Paleomagnetic field predictions were produced by Andreas Nilsson (Department of Geology, Lund University) using the paleomagnetic field models *pfm9k.1a* by Nilsson et al. (2014) and *A_FM* by Licht et al. (2013) for the coordinates 49.4º south 70.2º east.

5 Results

5.1 Stratigraphy

The following description of the sedimentary stratigraphy is based on visual inspection of the cores sub-sampled for magnetic measurements (Fig. 4).

5.1.1 Core L1-1

Core L1-1 extends from the lake floor to a depth of 1 meter. The uppermost 58 cm consists of massive silty clay with a few lenses of sandy silt. A slightly coarser unit consisting of sandy silty clay occurs at 58-75 cm. Massive silty clay is found below 75 cm, separated from the coarser unit by an erosional boundary.

Mosses, possibly of the species *Warnstofia fontinaliopsis* (Nathalie Van der Putten, pers. comm. 2016)

Table 2. Samples exposed to anhysteretic and isothermal remanent magnetizations.

Sample code	Core	Depth in core (cm)	Composite depth (cm)
L1-1_427	L1-1	42.7	42.7
L1-1_709	L1-1	70.9	70.9
L1-3_166	L1-3	16.6	89.6
L1-3_355	L1-3	35.5	108.5
L1-3_734	L1-3	73.4	146.4
L1-4_271	L1-4	27.1	165.1
L1-5_485	L1-5	48.5	257.5
L1-5_899	L1-5	89.9	298.9

are found throughout the core, but the moss content varies. Very few mosses are found in the uppermost 40 cm, whereas mosses are more abundant in the lower 60 cm.

5.1.2 Core L1-3

Core L1-3 is taken between 83 and 183 cm below the lake floor. A section between 83 and 177 cm consists of massive silty clay with the occurrence of a few thin layers of slightly coarser material, and two potential erosional boundaries at 155 respectively 173 cm. The bottom six centimeters consists of tephra (massive coarse sand). Mosses can be found throughout the silty clay. Between 113 and 153 cm, the moss content is very high, while it is relatively low from 153 to 177 cm.

5.1.3 Core L1-4

Core L1-4 is taken between 150 and 250 cm below the lake floor. Massive silty clay is found from 150 to 200 cm with the uppermost 10 cm resembling the L1-3 section with very high moss content. At 160 cm, an erosional boundary is found. Below the erosional boundary, the moss content decreases.

From 200 to 240 cm, massive tephra similar to that of core L1-3 is found. Below the tephra, massive silty clay with few mosses reappears to a depth of 245 cm where an erosional boundary separates it from laminated silty clay.

5.1.4 Core L1-5

Core L1-5 is taken between 219 and 319 cm below the lake floor. No sediment is found from 219 to 241 cm due to wash out. The washed out sediment probably consisted of tephra (coarse sand), since such sediment is found from 241 to 247 cm. From 247 to 319 cm, the core consists of laminated silty clay, with a few thin sandy layers. Mosses are very few within the laminated section, but are found in the sandy layers.

5.2 Core correlation

The core correlations shown in Fig. 4 are based on visually observed sedimentary stratigraphy and matching of the TAMISCAN magnetic susceptibility curves. The susceptibility curves of the overlapping sections of cores L1-1 and L1-3 do not match well. These cores are therefore correlated using core L1-2 as an intermediary.

Parts of the overlapping sections of cores L1-3 and L1-4 show similar patterns of susceptibility. Their similarity diminishes around a correlated depth of 165 cm. This might be explained by the occurrence of the potential erosional boundary in L1-3 at this depth. In both cores, silty clay with few mosses is found above the coarse sand, but the section containing few mosses is shorter in core L1-3, indicating the presence of a hiatus.

The cores L1-4 and L1-5 are correlated by the upper border of the laminated silty clay sections. There might be a hiatus in core L1-5 indicated by the lack of massive silty clay above the laminated section, as observed in core L1-4.

Based on the described correlations, a composite depth scale and a sedimentary log have been established (Fig. 5). On the composite depth scale, the bottom ten cm of core L1-3 has been shifted downwards so that the boundaries between silty clay and coarse sand in cores L1-3 and L1-4 are found at equal depth.

5.3 Radiocarbon dating

Table 3 shows the result of the radiocarbon dating. The radiocarbon dates have been calibrated with the CALIB 7.1 software using the SHcal13 calibration curve. The result indicates a calibrated age of -7 years BP at the top of sequence L3 and a calibrated age of 958/981 years BP at the bottom. Several reversals occur within the sequence, with apparently older sediment deposited above apparently younger sediment.

5.4 Magnetic measurements

5.4.1 Declination and inclination

The ChRM of a total of 153 discrete samples from sequence L1 were determined after visual inspection of their Zijderveld plots (Fig. 6). Most plots indicated the presence of a viscous remanent magnetization with release forces of 10 to 15 mT. The principal component analysis was in most cases based on the demagnetization steps from 15 to 80 mT, but individual ranges were chosen when this interval was considered inapplicable. The declination and inclination of the ChRM as well as maximum angular deviations (MAD) and angular deviations (AD) from the origin of all samples are shown in Fig. 7.

The quality of the data varies within the sequence reflected by relatively high MAD-values in cores L1-1 (<15°) and L1-3 (<16°) and relatively low MAD-values in cores L1-4 (<8°) and L1-5 (<5°). There are no defined MAD-values as indicators of reliable data, but MAD-values of less than 5° are considered reliable for Holocene marine sediments (Stoner & St-Onge 2007) and MAD-values in general of more than 15° are indicative of questionable data quality (Butler 1992).

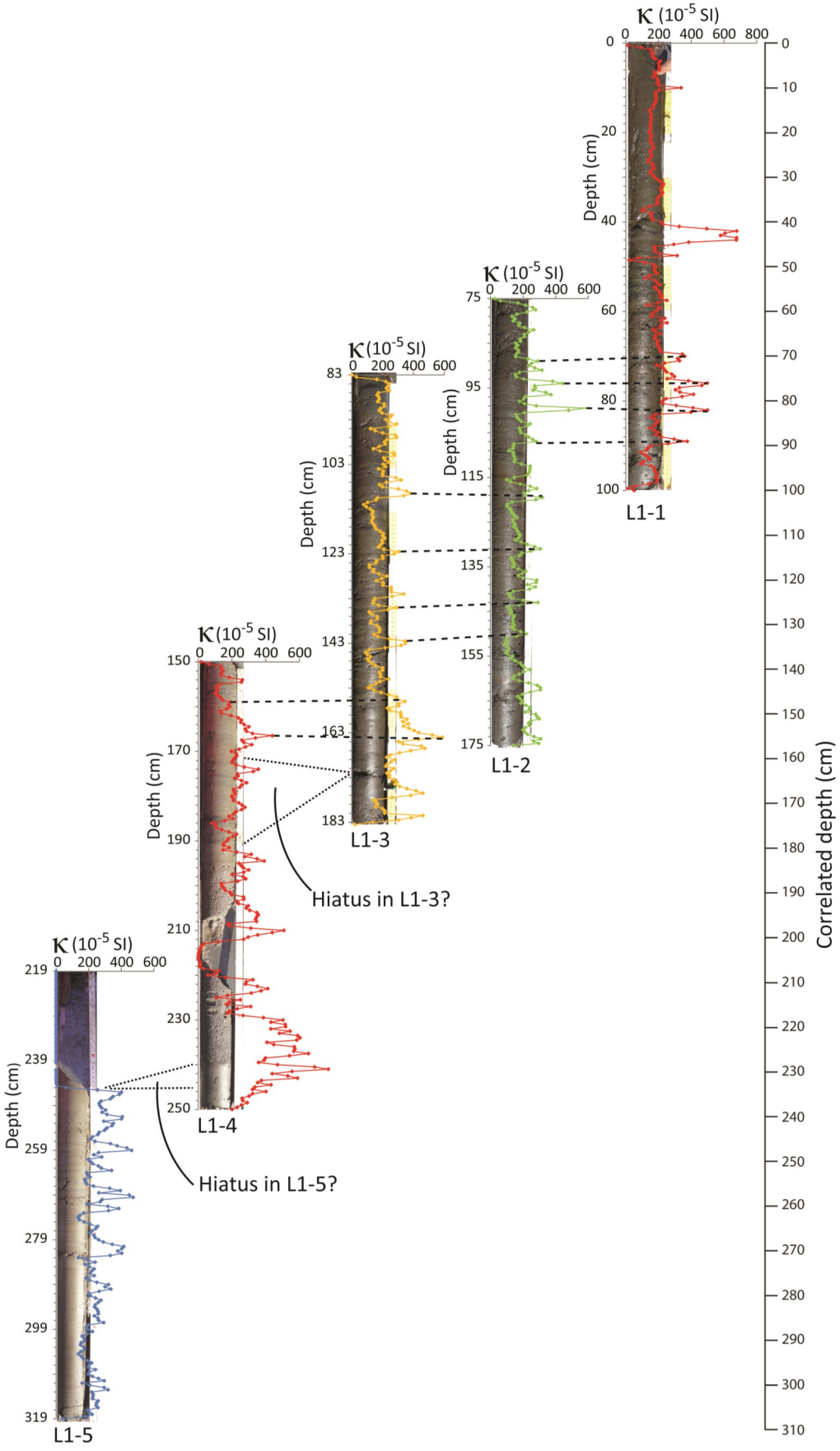

Fig. 4. Correlation of the cores L1-1, L1-2, L1-3, L1-4 and L1-5 based on matching of TAMISCAN magnetic susceptibility (κ) curves. Dashed lines show peak-to-peak visual correlations.

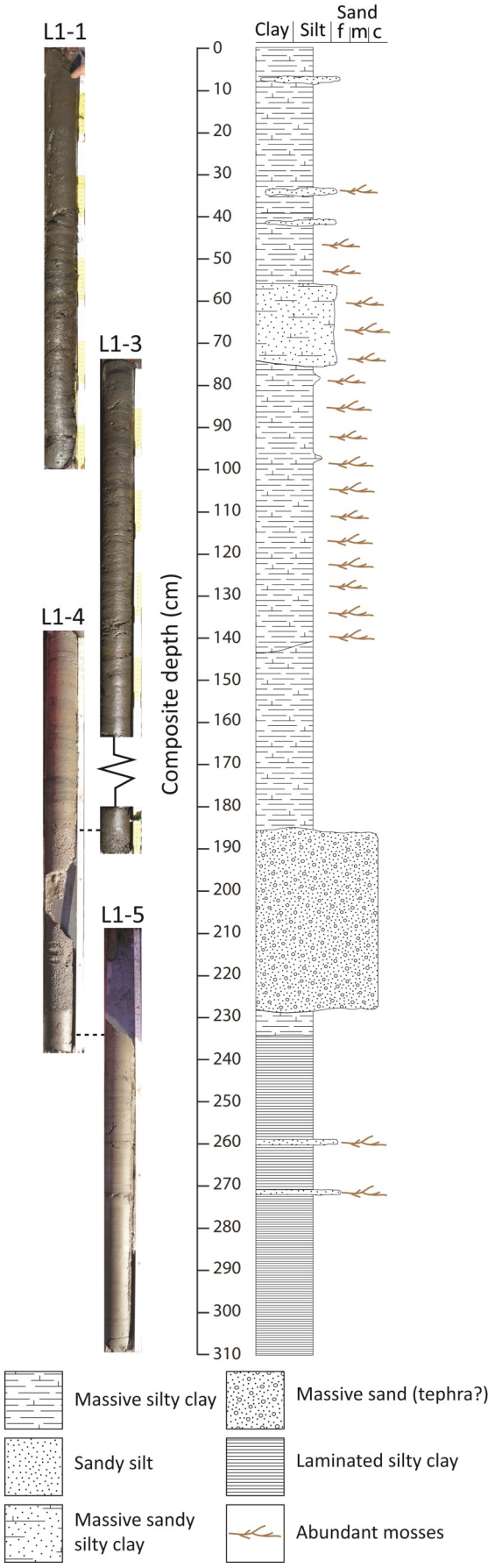

Fig. 5. Composite log based on the sedimentary stratigraphy of the cores L1-1, L1-3, L1-4 and L1-5.

5.4.2 Magnetic properties

Fig. 8 shows the demagnetization curve of the ARM imparted on the eight subsamples described in Table 2 with normalized ARM intensities. The demagnetization curves are similar in appearance for all samples, and indicate a mean destructive field (MDF_{ARM}) of approximately 20 *mT*. The SIRM imparted at 1*T* and the IRM imparted in the opposite direction at -300 *mT* are shown in Table 4. Due to technical difficulties, three of the eight samples were unfortunately given an IRM of a wrong direction. The S-ratio for the five remaining samples, calculated as $IRM_{-300\ mT}/\ SIRM_{1\ T}$, show values around -0.97, indicating a magnetic mineral assemblage of mainly low coercivity minerals (Stoner & St-Onge 2007).

5.5 Paleomagnetic field predictions

The predicted inclination values for the time-period from -60 to 2000 years BP according to the two models *pfm9k.1a* and *A_FM* are generally in accordance (Fig. 9A). Both models indicate a period of relative steady inclination from 2000 to 1300 years BP followed by an inclination shallowing to a minimum inclination of approximately -45º. From 1300 years BP to the present, *pfm9k.1a* indicates a second period of steady inclination, while *A_FM* shows a more complex variation in inclination.

The models are in less agreement concerning declination values over the same time span as mentioned above (Fig. 9B). The *pfm9k.1a* model suggests a period of relative constant declination lasting from 2000 to 800 years BP followed by a westward shift in declination that changes to an eastward shift at around 300 years BP. In disagreement with the constant declination predicted by *pfm9k.1a*, the *A_FM* model shows three distinctive declination features around 1800, 1400 and 800 years BP followed by a more or less continuous westward shift in declination from 800 to -60 years BP.

6 Discussion

6.1 Magnetic mineral content

It is not possible to determine the makeup of the magnetic mineral content of the lake sediment based on the magnetic measurements of this study. Studies of the basalts of the Kerguelen archipelago have revealed a widespread occurrence of titanomagnetites (Gautier et al. 1990), providing a likely candidate for the ChRM carrier of the sediment.

The S-ratios of the samples that were successfully examined were all close to -1. Though a general conclusion cannot be based on just five samples, the S-

Table 3. Radiocarbon dates obtained from sediment sequence L3. Dates have been transferred to approximate depth on the L1 composite depth scale (see Fig. 5) by correlation of stratigraphic boundaries and TAMISCAN magnetic susceptibility pattern matching. Samples with LuS codes were dates at the Single Stage AMS at Lund University. Samples with SacA codes were dates at the CEA Saclay in France.

Code	Core	Depth below lake floor (cm)	Depth on L1 composite scale (cm)	Uncalibrated ^{14}C-age (years BP)	Calibrated age[a] (years BP)	Material
LuS 11218	L3-1	12	12	1.040 ± 0.004 Fm[b]	-7	Bulk
SacA 43303	L3-1	48	48	1030 ± 30	869	Bulk
SacA 43304	L3-2	85	75	635 ± 30	605	Mosses
LuS 11219	L3-2	125	119	665 ± 40	605	Mosses
SacA 43305	L3-3	172	138	720 ± 30	633	Mosses
SacA 43306	L3-3	222	235	665 ± 30	606	*Azorella*
LuS 11055	L3-4	262	272	1020 ± 35	863	*Azorella*
SacA 43307	L3-4	274	283	2230 ± 30	2225	Bulk
LuS 11220	L3-4	292	300	1210 ± 35	1068	*Azorella*
LuS 11036	L3-4	306	315	1100 ± 35	958	*Azorella*
LuS 11098	L3-4	306	315	1125 ± 30	981	*Azorella*

[a]Median probability based on calibrations using the SHcal13 calibration curve with the CALIB 7.1 software
[b]Fraction modern

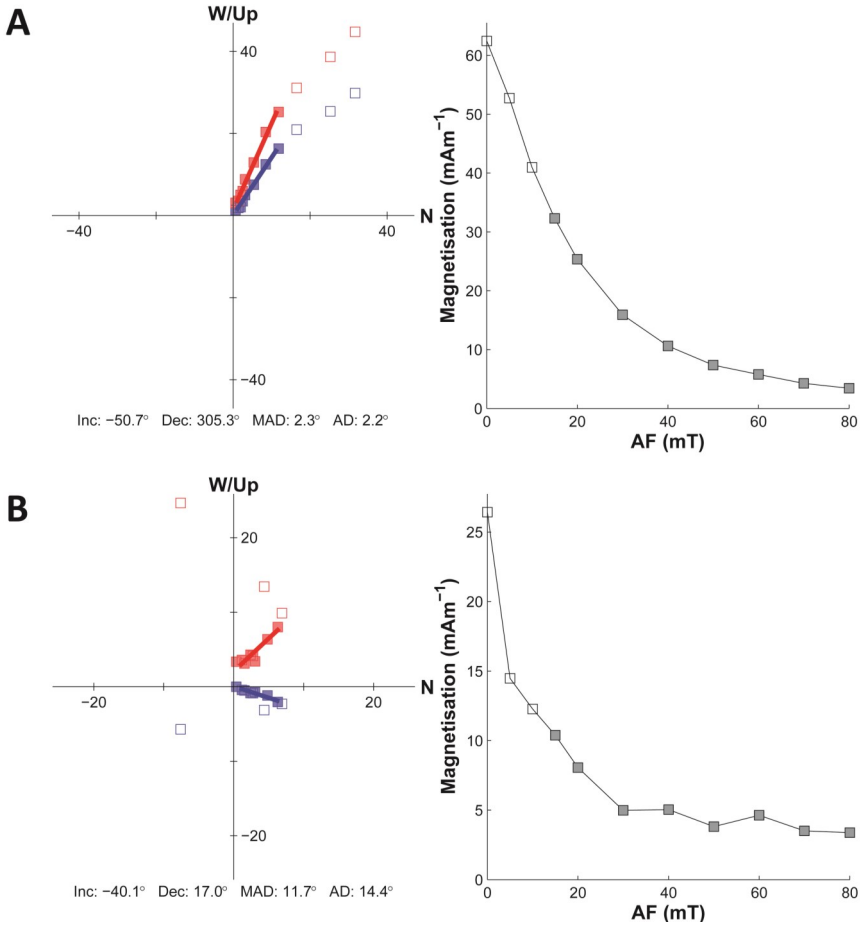

Fig. 6. Zijderveld plots and demagnetization curves for data of high (**A**) respectively low (**B**) quality. Blue vectors represent projections of the ChRM onto the horizontal plane while red vectors represent projections onto the vertical plane. The axis labels N (north) and W (west) apply for blue vectors, while the axis label Up applies for red vectors. Open boxes indicate the presence of a secondary component of the remanent natural magnetization, while closed boxes represent the demagnetization steps considered for the calculation of the characteristic remanent magnetization.

ratios indicate a presence of mainly magnetic minerals with low release forces such as (titano-)magnetite (e.g. Stoner & St-Onge 2007). The appearance of the ARM demagnetization curves (Fig. 8) and the average MDF around 20 mT also indicates magnetite being the main magnetic mineral as these are in accordance with typical demagnetization curves and MDF-levels for magnetite suggested by Peters & Thompson (1998).

Table 4. Saturation isothermal remanent magnetisation (SIRM) at field of 1 T, isothermal remanent magnetization at a backfield of -300 mT and the S-ratio of eight subsamples.

Sample code	$SIRM_{1\ T}$ (A/m)	$IRM_{-300\ mT}$ (A/m)	S-ratio
L1-1_427	32.62	-31.53	-0.97
L1-1_709	10.58	*N/A*	*N/A*
L1-3_166	9.98	-9.68	-0.97
L1-3_355	9.83	*N/A*	*N/A*
L1-3_734	13.63	*N/A*	*N/A*
L1-4_271	13.00	-12.66	-0.97
L1-5_485	14.41	-14.00	-0.97
L1-5_899	11.62	-11.17	-0.96

6.2 Declination and inclination

Prior to interpretation, outliers and data points with MAD and AD-values greater than 10º respectively 15º were removed. The average inclination of the remaining data set is -52º, approximately 14 degrees shallower than the expected inclination for the latitude according to the GAD hypothesis. There are several plausible explanations for this observation. Inclination error is a commonly observed phenomenon in both natural deposition of sediments and in re-deposition experiments (Tauxe & Kent 1984). Inclination error results in too shallow inclinations compared to the applied external magnetic field, and might explain the shallow inclinations observed in Lake Cocytus. Furthermore, the GAD hypothesis is based on the alignment of the geomagnetic dipole with Earth's rotational axis averaged over time. It is plausible that the time span of the sediment sequence is too short to allow for satisfactory calculation of expected inclination according to the GAD hypothesis.

While the average observed inclination might be reconciled with the GAD hypothesis, some observed values are unreasonable for the Kerguelen Islands. Inclinations indicative of a location at the magnetic equator are found at a composite depth of around 75

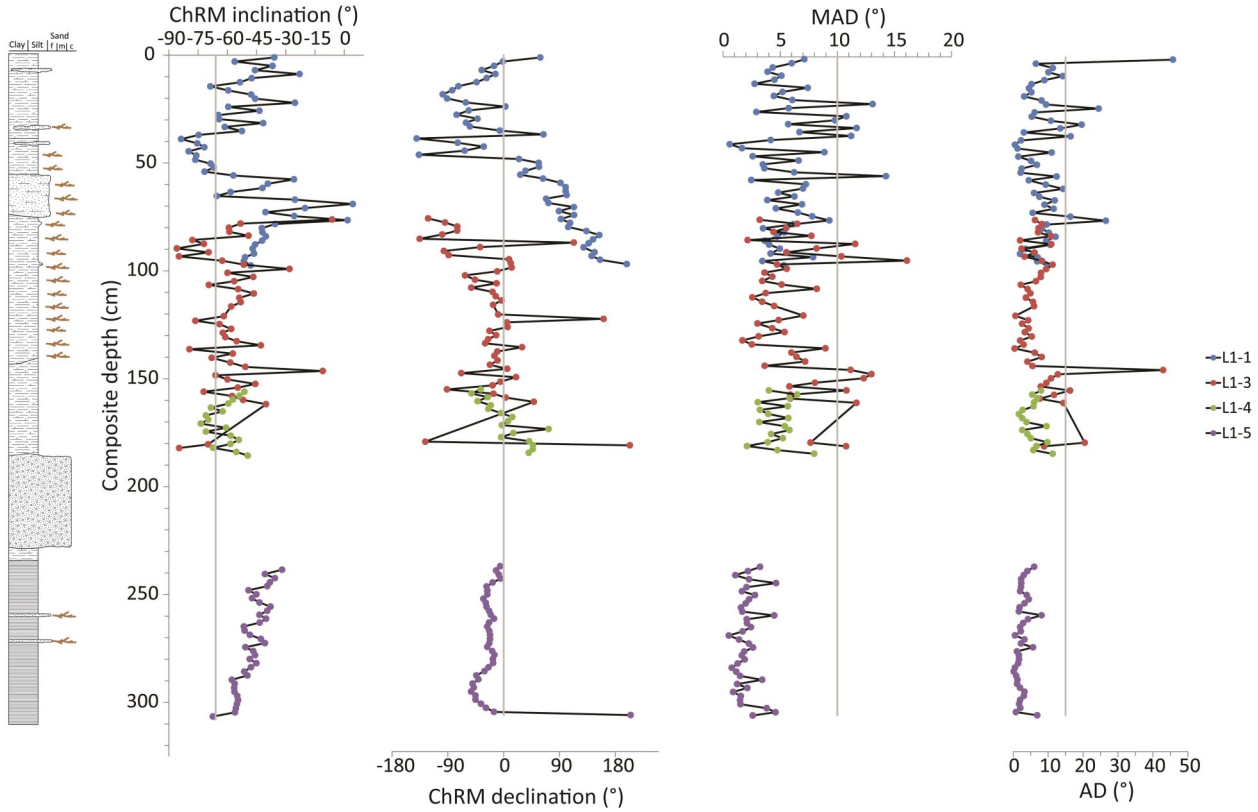

Fig. 7. **A**. Inclination, declination maximum angular deviation (MAD) and angular deviation (AD) for the characteristic remanent magnetization (ChRM) of the cores L1-1, L1-3, L1-4 and L1-5 plotted on a composite depth scale. Gray lines from left to right represent the expected inclination according to the geocentric axial dipole hypothesis, the average relative declination, a MAD-level of 10º and an AD level of 15º.

cm seem unreasonable to have come about by paleosecular variations. Furthermore, the paleomagnetic data of overlapping core sections would be expected to be nearly identical, provided that the core correlations are reliable. From Fig. 7 it is clear that neither inclination nor declination of the overlapping sections of the cores L1-1 and L1-3 are the same. The declinations of both cores show a westward drift, but their values differ by about 180 to 200º. Due to the nature of the Russian corer, it is possible that the discrepancy could be explained by an azimuth difference of 180º when retrieving core L1-1 relative to the other cores, but this must be considered unlikely, and would introduce further complications.

The explanation of the above mentioned inconsistencies is likely found in processes governing the deposition of the sediment.

6.3 Slump deposit hypothesis

One hypothesis that might be able to explain the discrepancies between cores and the occurrence of sections with questionable inclination and declination patterns is that a section of the sequence consists of one or more sediment packages deposited by slump processes. Reworking of the sediment during slumping could account for inclinations and declinations that do not reflect paleosecular variation.

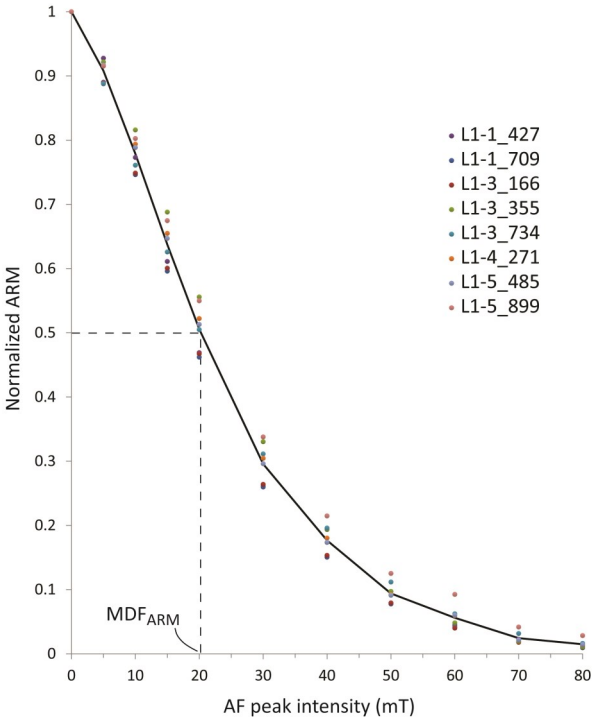

Fig. 8. Demagnetization curve of the anhysteretic remanent magnetization (ARM) imparted on eight samples in an alternating field (AF) of 80 mT and a bias field of 0.05 mT. The ARM of each sample is normalized to the samples maximal ARM value. The black line indicates the average demagnetization curve. The dashed line indicates and average median destructive field of the ARM (MDF$_{ARM}$) of approximately 20 mT.

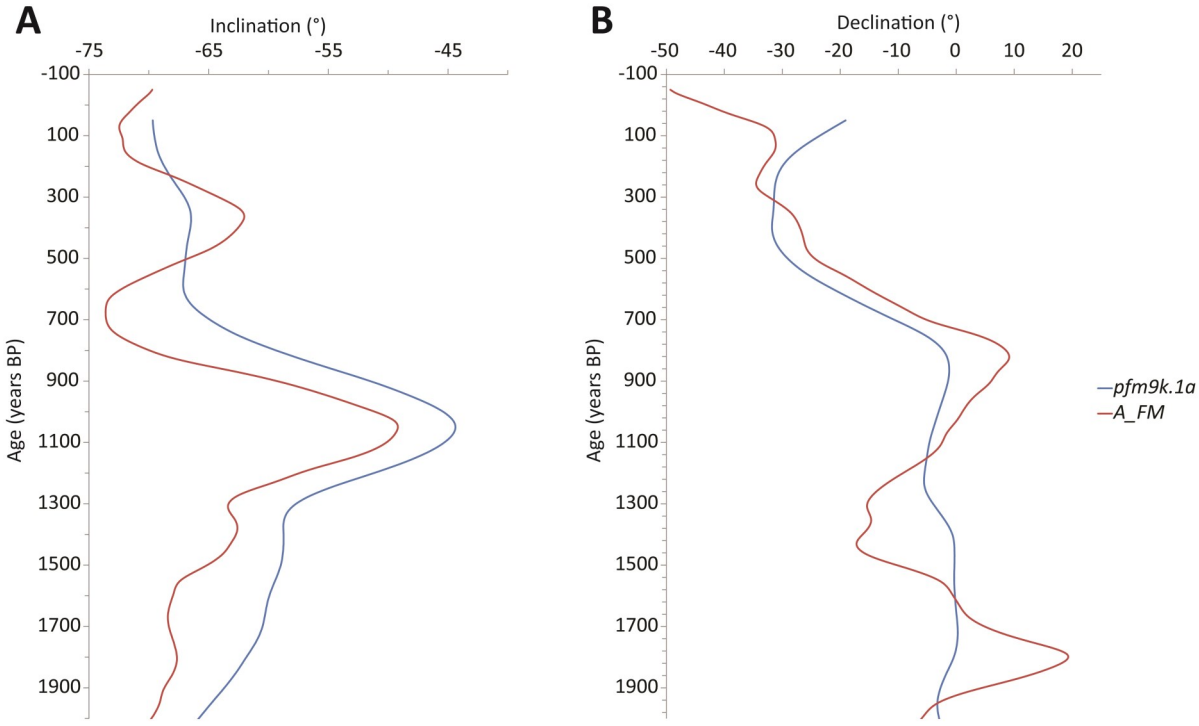

Fig. 9. Inclination (**A**) and declination (**B**) at 49.4º south and 70.2º east from present day to 2000 years before present (BP) as predicted by the two paleomagnetic models *pfm9k.1a* and *A_FM*.

The occurrence of abundant mosses in parts of cores L1-1 and L1-3 supports this notion. According to Ochyra et al. (2008) *W. fontinaliopsis* grows in moist or wet habitats. It is often found at the margins of lakes, and more rarely below water down to a maximum depth of four meters. If the mosses found in the sequence are indeed *W. fontinaliopsis*, it is feasible that they grew on the shallow platforms along the lake margin, and were relocated to a greater depth via slumping. However, without knowing past water level fluctuations, we cannot rule out that the mosses grew in situ at a time of lower water level, but the radiocarbon dates suggests a slump deposit scenario.

The radiocarbon dates indicate that the sediment at a composite depth of 235 cm is of approximately the same age as the sediment at a composite depth of 75 cm. This infers an unreasonably high accumulation rate, unless the sediment consists of several packages of approximately equal age that were deposited during a slumping event. The apparent age reversal at a composite depth of 138 cm is also in agreement with a slump hypothesis, since slumping might involve the relocation of older sediment originally deposited upslope. However, the uncertainties of the radiocarbon dates does allow for an interpretation that does not include the occurrence of an age reversal. Not all apparent age reversals within the sequence are thought to be indicative of slumping. Bulk samples are known to overestimate ages due to the presence of older minerogenic carbon or reworked older organic material (Björck & Wohlfarth 2001). The apparent age reversal at a composite depth of 283 cm as inferred by dating of a bulk sample is probably a product of reworking of older organic material, since the laminated texture of the sediment at the same depth suggests a sequence of undisturbed sediment. It is more difficult to explain the apparent age reversal indicated a sample of *A. selago* within the same laminated section, but a interpretation that excludes an age reversal is reasonable within the uncertanties of the radiocarbon dates.

Slumps are known to be triggered by earthquakes, as evident by the slump deposits linked to earthquakes in Lake Lucerne (Switzerland) by Schnellmann et al. (2002). The Kerguelen archipelago is a volcanically active area, and though the Kerguelen plateau is classified as an aseismic ridge (Adams & Zhang 1984), earthquakes do occur there. The morphology of the lake with its steep floor leading to the coring site and the occurrence of earthquakes within the area bring further plausibility to the slump deposit hypothesis.

Determining the extent of the potential slump deposits within the sequence is not straightforward, but under the assumption that abundance of mosses is indicative of slumped material from shallower areas of the lake, the part of the sequence affected by slumping is constrained to 1.2 meters of sediment from 30 to 150 cm depth on the composite depth scale.

6.4 Age-depth model

In an attempt to establish an age-depth model, the data of the parts of sequence L1 assumed to be in situ has been compared to the paleomagnetic model predictions (Fig. 10), of which the *A_FM* models shows the greatest similarity. Four inclination features and three declination features show possible correlation with the data from the cores L1-4 and L1-5 for the period 700 to 1550 years BP, while the data from core L1-1 shows no similarity with either of the models. The inability to match the data from core L1-1 with the models might be explained by the fact that it is obtained from sediment immediately below the lake floor where postdepositional magnetization processes still might be ongoing. It is also possible that the uppermost sediment has been affected during the coring process to a greater extent than the more compacted and dewatered sediments found at greater depths.

Uncertainty concerning the correlation of the features exists. This is especially true for the two questionable features I? and D? which are based exclusively on pattern appearance and for I-2 located at the core break of L1-5, as it coincides with the presumed hiatus between cores L1-4 and L1-5.

An age-depth model for the lower half of sequence L1 obtained by linear interpolation between the suggested features, shows some discrepancies with the radiocarbon dates inferred from sequence L3 (Fig. 11). A plausible age-depth model based on a liberal interpolation between the existing non-bulk radiocarbon dates and on the presumption that slump material occur above a composite depth of 150 cm is shown in Fig. 11 as well. The paleomagnetic age-depth model is generally in accordance with a liberal interpretation of the radiocarbon dates concerning accumulation rates, but indicates systematically older ages by several hundred years. This is in opposition to what might be expected due to delay of the acquisition of the remanent magnetization, since a delay results in apparent younger ages as shown by Suganuma et al. (2010).

There is little reason to doubt the validity of the radiocarbon dates, except for the dates based on bulk material. The apparent age reversal around a composite depth of 300 cm in what presumably is in situ sediment, might be explained by studying the probability curves in Fig. 11. The probability curve for the apparent reversal date covers a wide time span, and it is

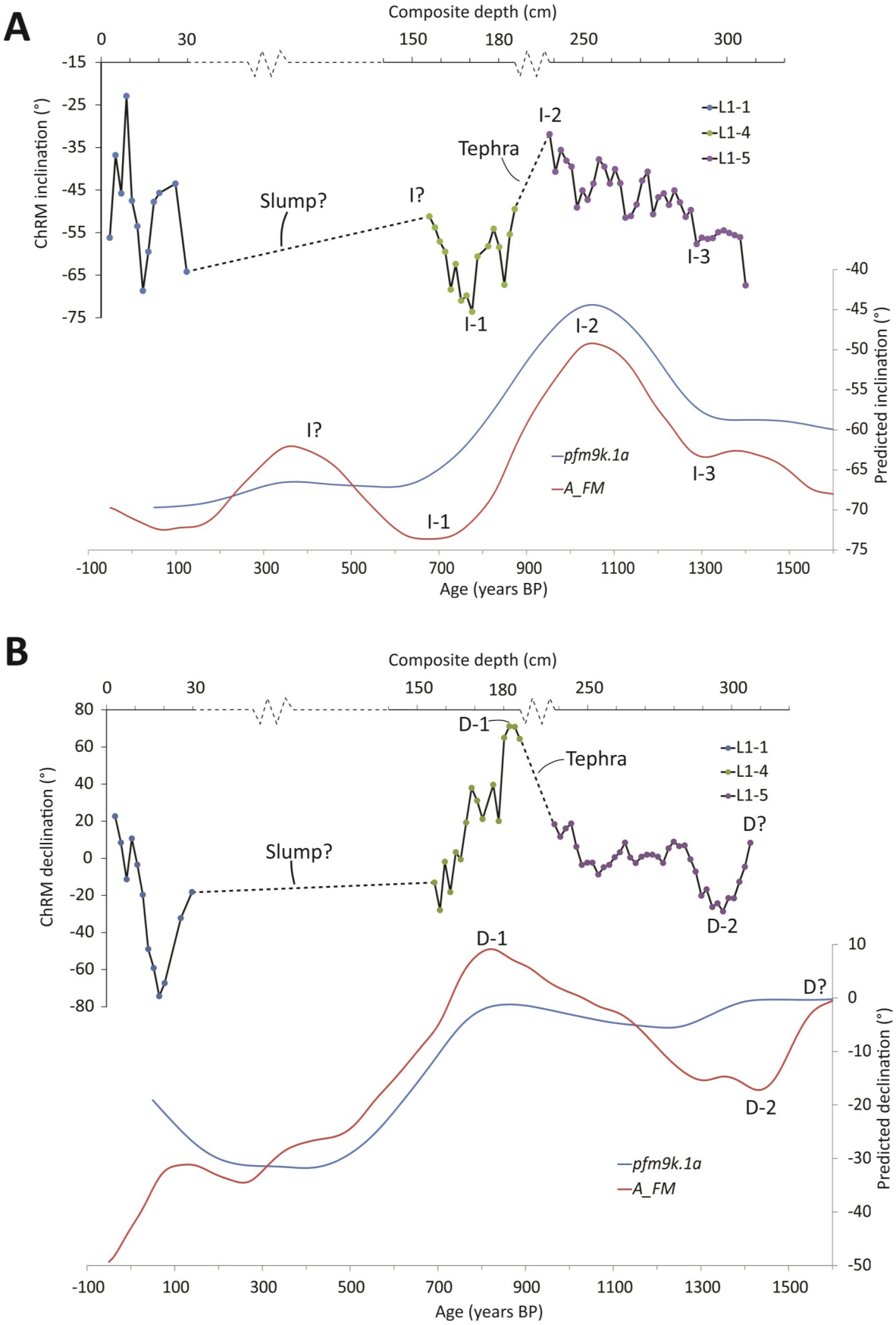

Fig. 10. Comparison of inclination (**A**) and declination (**B**) data from sediment presumed to be in situ with predicted values according to the paleomagnetic models *pfm9k.1a* and *A_FM* with identification of suggested inclination- and declination features. Note that observed and predicted values are plotted on different scales.

possible to make an interpretation of the carbon dates that does not include a reversal.

Rather than the radiocarbon dates being unreliable, it seems more likely that the inconsistencies between the radiocarbon dates and the paleomagnetic age-depth model arise from limitations of the paleomagnetic models, errors introduced during laboratory work or from uncertainties in the interpretation of the data.

6.5 Reliability of the paleomagnetic field models

The *A_FM* model to which the data set showed certain similarities is based on a dataset of archeomagnetic data obtained from igneous rocks and archeological material, with only a 2.5% contribution from the southern hemisphere (Licht et al. 2013). The *pfm9k.1a* model incorporates sedimentary as well as archeomagnetic data, but is also heavily overrepresented by data from the northern hemisphere. Considering the spatial limitations of the data sets and the complexity of the geomagnetic field, it is not unreasonable to think that the apparent offset between the age-depth model and the radiocarbon dates are due to uncertanties in the paleomagnetic field models. A plausible explanation for such an offset could be found in the potential existence of a regional magnetic field anomaly in the Indian Ocean around this time, similar to the South Atlantic magnetic anomaly (see Hartmann & Pacca 2009).

6.6 Complementary studies

In order to successfully establish a reliable age-depth model for the lake sequences, it is recommended to obtain additional non-bulk samples for radiocarbon dating from a few selected key horizons. Dating of a sample from core L1-4 at a in-core depth around of 12 cm (composite depth 150 cm) would provide insight into the upper limit of the sediment presumed to be in situ. Samples from the same core obtained within a few centimeters on either side of the tephra layer would shed light on the existence of a hiatus, and so would samples from core L1-3 at in-core depths of around 87 cm and 90 cm (composite depths of 160 cm and 183 cm). A sample core L1-1 at an in-core depth of 20 to 30 cm would also be of interest, since only bulk samples has been obtained from the uppermost part of the sediment sequences.

At the time of writing, effort is being made to establish the first Holocene tephrochronology of the Kerguelen archipelago by a team of scientists (Leloup Besson et al. 2016). If a tephrochronology is successfully established, a tephrochronological study of the sediment sequence could further strengthen the chronology.

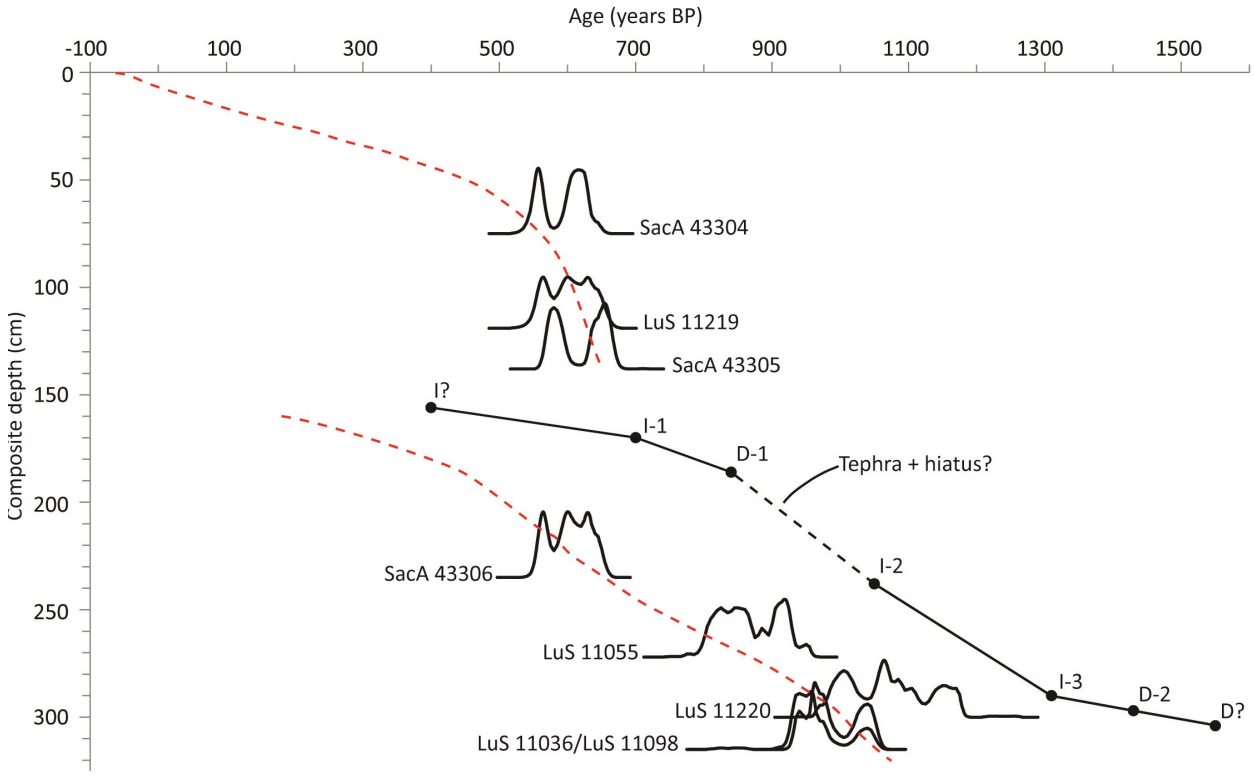

Fig. 11. Black line: Age-depth model for the lower half of sequence L1 based on linear interpolation between inclination and declinations feature as shown in Fig. 10. Red dashed line: A potential age-depth model based on a liberal interpolation between the probability curves for radiocarbon dates (see Table 3) and on the presumption that slump material occur above a composite depth of 150 cm. .

6.7 Sources of error

Though care was taken during subsampling, introduction of errors in the procedure cannot be disregarded. Errors during the pre-cutting could occur from either physical reorientation of mineral grains due to friction or from magnetic alteration due to the weak magnetic field of the knife. Physical reorientation of grains is deemed more likely in core sections with abundant mosses. Whether this is the explanation for the generally lower data quality of such sections remains unknown.

7 Conclusions

Magnetic measurements of the cores L1-1, L1-3, L1-4 and L1-5 revealed the presence of a two-component remanent magnetization. The ChRM was generally isolated after AF demagnetization with peak intensity of 10-15 mT. Inconsistencies between the ChRM overlapping parts of cores, age reversals inferred by radiocarbon dating and the presence of abundant mosses within core sections indicate that sections of the sequence might consist of slump deposits. Investigation of the ChRM of parts of the sequence presumed to be in situ reveal similar features to those of the *A_FM* paleomagnetic model, but a simple age-depth model based on comparison with the paleomagnetic model indicate ages that conflict with the radiocarbon dates obtained from sequence L3. The inconsistencies are likely due to spatial limitations of the paleomagnetic field models or the interpretation of the data.

To improve the understanding of the chronology of the sediment sequence, complementary studies comprising radiocarbon dating of a few selected key horizons are recommended.

8 Acknowledgements

I would like to thank my supervisors for giving me the opportunity to test the paleomagnetic method. I would like to thank Andreas Nilsson for his patience with me and for always keeping the door open, and Nathalie Van der Putten for her helpfulness and for letting me sample her hard-earned cores. I am grateful to my wife, Ashley Noel Hulcoop, for excellent editorial advice. Lastly, I would like to thank my fellow bachelor students from the department of geology for keeping up the good spirit during the writing process.

9 References

Adams, R. D. & Zhang, B. M., 1984: A further earthquake on the Kerguelen plateau. *Geophysical Journal of the Royal Astronomical Society 79*, 697-703.

Barletta, F., St-Onge, G., Channell, J. E. T. & Rochoria, A., 2010: Dating of Holocene western Canadian Arctic sediments by matching paleomagnetic secular variation to a geomagnetic field model. *Quaternary Science Reviews 29*, 2315-2324.

Benard, F., Callot, J.-P., Vially, R., Schmitz, J., Roest, W., Patriat, M., Loubrieu, B. & Extraplac, T., 2010: The Kerguelen plateau: Records from a long-living/composite microcontinent. *Marine and Petroleum Geology 27*, 633-649.

Björck, S. & Wohlfarth, B. 2001: ^{14}C chronostratigraphic techniques in paleolimnology. *In* W. M. Last & J. P. Smol (red.): *Tracking Environmental Change Using Lake Sediments. Volume 1: Basin Analysis, Coring, and Chronological Techniques*, 205-246. Kluwer Acedemic Publishers, Dordrecht.

Butler, R. F., 1992: *Paleomagnetism: Magnetic Domains to Geologic Terranes*. Blackwell Scientific Publications, Boston.

Cogley, J. G., Berthier, E. & Donoghue, S. 2014: Remote Sensing of Glaciers of the Subantarctic Islands. *I* J. S. Kargel, G. J. Leonard, M. P. Bishop, A. Kääb & B. H. Raup (red.): *Global Land Ice Measurements from Space*, 759-780. Springer,

Constable, C. G. & Constable, S. C. 2004: Satellite magnetic field measurements: Applications in studying the deep Earth. *In* R. S. J. Sparks & C. J. Hawkesworth (red.): *State of the Planet: Frontiers and Challenges in Geophysics*, 147-159.

Damasceno, D., Scoates, J. S., Weis, D., Frey, F. A. & Giret, A., 2002: Mineral chemistry of mildly alkalic basalts from the 25 Ma Mont Crozier section, Kerguelen Archipelago: Constraints on phenocryst crystallization environments. *Journal of Petrology 43*, 1389-1413.

Fernandez, M., Bjorck, S., Wohlfarth, B., Maidana, N. I., Unkel, I. & Van der Putten, N., 2013: Diatom assemblage changes in lacustrine sediments from Isla de los Estados, southernmost South America, in response to shifts in the southwesterly wind belt during the last deglaciation. *Journal of Paleolimnology 50*, 433-446.

Gautier, I., Weis, D., Mennessier, J. P., Vidal, P., Giret, A. & Loubet, M., 1990: Petrology and geochemistry of the Kerguelen archipelage basalts (South Indian Ocean) - Evolution of the mantle sources from ridge to intraplate position. *Earth and Planetary Science Letters 100*, 59-76.

Hall, K., 1984: Evidence in favor of an extensive ice cover on sub-Antarctic Kerguelen island during the last glacial. *Palaeogeography Palaeoclimatology Palaeoecology 47*, 225-232.

Hartmann, G. A. & Pacca, I. G., 2009: Time evolution of the South Atlantic Magnetic Anomaly: *Anais Da Academia Brasileira De Ciencias 81*, 243-255.

Kirschvink, J. L., 1980: The least-squares line and plane and the analysis of paleomagnetic data. *Geophysical Journal of the Royal Astronomical Society 62*, 699-718.

Leloup Besson, A., Sabatier, P., Moine, B., Poulenard, J., Malet, E., Fanget, B., Develle, A., L., Storen, E., Bakke, J. & Arnaud, F., 2016: Établissement de la première chronologie Holocène des éruptions dans l'archipel des Kerguelen. *12èmes Journées Scientifiques du CNFRA (Comité National Français des Recherches Arctiques et Antarctiques)*. Lyon, France.

Licht, A., Hulot, G., Gallet, Y. & Thebault, E., 2013: Ensembles of low degree archeomagnetic field models for the past three millennia. *Physics of the Earth and Planetary Interiors 224*, 38-67.

Lisiecki, L. E. & Raymo, M. E., 2005: A Pliocene-Pleistocene stack of 57 globally distributed benthic delta O-18 records. *Paleoceanography 20*.

Nilsson, A., Holme, R., Korte, M., Suttie, N. & Hill, M., 2014: Reconstructing Holocene geomagnetic field variation: new methods, models and implications: *Geophysical Journal International 198*, 229-248.

Ochyra, R., Smith, R. I. L. & Bednarek-Ochyra, H., 2008: *The Illustrated Moss Flora of Antarctica*. Cambridge Univsersity Press, New York. 685 pp.

Peters, C. & Thompson, R., 1998: Magnetic identification of selected natural iron oxides and sulphides: *Journal of Magnetism and Magnetic Materials 183*, 365-374.

Schnellmann, M., Anselmetti, F. S., Giardini, D., Mckenzie, J. A. & Ward, S. N., 2002: Prehistoric earthquake history revealed by lacustrine slump deposits: *Geology 30*, 1131-1134.

Stoner, J. S. & St-Onge, G. 2007: Magnetic stratigraphy in paleoceanography: Reversals, excursions, paleointensity, and secular variation. *In* C. Hillaire-Marcel & A. De Vernal (red.): *Developments in Marine Geology*, 99-138. Elsevier B. V.

Suganuma, Y., Yokoyama, Y., Yamazaki, T., Kawamura, K., Horng, C.-S. & Matsuzaki, H., 2010: 10Be evidence for delayed acquisition of remanent magnetization in marine sediments: Implication for a new age for the Matuyama–Brunhes boundary: *Earth and Planetary Science Letters 296*, 443-450.

Tauxe, L. & Kent, D. V., 1984: Properties of a detrital remanence carried by hematite from study of modern river deposits and laboratory experiments: *Geophysical Journal of the Royal Astronomical Society 76*, 543-561.

Thompson, R. & Oldfield, F., 1982: *Environmental Magnetism*. Allen & Unwin Ltd, London. 227 pp.

Van der Putten, N., Verbruggen, C., Bjorck, S., Michel, E., Disnar, J.-R., Chapron, E., Moine, B. N. & De Beaulieu, J.-L., 2015: The Last Termination in the South Indian Ocean: A unique terrestrial record from Kerguelen Islands (49 degrees S) situated within the Southern Hemisphere westerly belt: *Quaternary Science Reviews 122*, 142-157.

Zijderveld, J. D. A. 1967: A. C. demagnetization of rocks: Analysis of results. *In* D. W. Collinson, K. M. Creer & S. K. Runcorn (red.): *Methods in paleomagnetism* 254-286. Elsevier Publishing Company, Netherlands.

Tidigare skrifter i serien ”Examensarbeten i Geologi vid Lunds universitet”:

429. Sjunnesson, Alexandra, 2015: Spårämnesförsök med nitrat för bedömning av spridning och uppehållstid vid återinfiltrationav grundvatten. (15 hp)
430. Henao, Victor, 2015: A palaeoenvironmental study of a peat sequence from Iles Kerguelen (49° S, Indian Ocean) for the Last Deglaciation based on pollen analysis. (45 hp)
431. Landgren, Susanne, 2015: Using calcein-filled osmotic pumps to study the calcification response of benthic foraminifera to induced hypoxia under *in situ* conditions: An experimental approach. (45 hp)
432. von Knorring, Robert, 2015: Undersökning av karstvittring inom Kristianstadsslättens NV randområde och bedömning av dess betydelse för grundvattnets sårbarhet. (30 hp)
433. Rezvani, Azadeh, 2015: Spectral Time Domain Induced Polarization - Factors Affecting Spectral Data Information Content and Applicability to Geological Characterization. (45 hp)
434. Vasilica, Alexander, 2015: Geofysisk karaktärisering av de ordoviciska kalkstensenheterna på södra Gotland. (15 hp)
435. Olsson, Sofia, 2015: Naturlig nedbrytning av klorerade lösningsmedel: en modellering i Biochlor baserat på en fallstudie. (15 hp)
436. Huitema, Moa, 2015: Inventering av föroreningar vid en brandövningsplats i Linköpings kommun. (15 hp)
437. Nordlander, Lina, 2015: Borrningsteknikens påverkan vid provtagning inför dimensionering av formationsfilter. (15 hp)
438. Fennvik, Erik, 2015: Resistivitet och IP-mätningar vid Äspö Hard Rock Laboratory. (15 hp)
439. Pettersson, Johan, 2015: Paleoekologisk undersökning av Triberga mosse, sydöstra Öland. (15 hp)
440. Larsson, Alfred, 2015: Mantelplymer - realitet eller *ad hoc*? (15 hp)
441. Holm, Julia, 2015: Markskador inom skogsbruket - jordartens betydelse (15 hp)
442. Åkesson, Sofia, 2015: The application of resistivity and IP-measurements as investigation tools at contaminated sites - A case study from Kv Renen 13, Varberg, SW Sweden. (45 hp)
443. Lönsjö, Emma, 2015: Utbredningen av PFOS i Sverige och världen med fokus på grundvattnet – en litteraturstudie. (15 hp)
444. Asani, Besnik, 2015: A geophysical study of a drumlin in the Åsnen area, Småland, south Sweden. (15 hp)
445. Ohlin, Jeanette, 2015: Riskanalys över pesticidförekomst i enskilda brunnar i Sjöbo kommun. (15 hp)
446. Stevic, Marijana, 2015: Identification and environmental interpretation of microtextures on quartz grains from aeolian sediments - Brattforsheden and Vittskövle, Sweden. (15 hp)
447. Johansson, Ida, 2015: Is there an influence of solar activity on the North Atlantic Oscillation? A literature study of the forcing factors behind the North Atlantic Oscillation. (15 hp)
448. Halling, Jenny, 2015: Inventering av sprickmineraliseringar i en del av Sorgenfrei-Tornquistzonen, Dalby stenbrott, Skåne. (15 hp)
449. Nordas, Johan, 2015: A palynological study across the Ordovician Kinnekulle. (15 hp)
450. Åhlén, Alexandra, 2015: Carbonatites at the Alnö complex, Sweden and along the East African Rift: a literature review. (15 hp)
451. Andersson, Klara, 2015: Undersökning av slugtestsmetodik. (15 hp)
452. Ivarsson, Filip, 2015: Hur bildades Bushveldkomplexet? (15 hp)
453. Glommé, Alexandra, 2015: $^{87}Sr/^{86}Sr$ in plagioclase, evidence for a crustal origin of the Hakefjorden Complex, SW Sweden. (45 hp)
454. Kullberg, Sara, 2015: Using Fe-Ti oxides and trace element analysis to determine crystallization sequence of an anorthosite-norite intrusion, Älgön SW Sweden. (45 hp)
455. Gustafsson, Jon, 2015: När började plattektoniken? Bevis för plattektoniska processer i geologisk tid. (15 hp)
456. Bergqvist, Martina, 2015: Kan Ölands grundvatten öka vid en uppdämning av de utgrävda dikena genom strandvallarna på Ölands östkust? (15 hp)
457. Larsson, Emilie, 2015: U-Pb baddeleyite dating of intrusions in the south-easternmost Kaapvaal Craton (South Africa): revealing multiple events of dyke emplacement. (45 hp)

458. Zaman, Patrik, 2015: LiDAR mapping of presumed rock-cored drumlins in the Lake Åsnen area, Småland, South Sweden. (15 hp)
459. Aguilera Pradenas, Ariam, 2015: The formation mechanisms of Polycrystalline diamonds: diamondites and carbonados. (15 hp)
460. Viehweger, Bernhard, 2015: Sources and effects of short-term environmental changes in Gullmar Fjord, Sweden, inferred from the composition of sedimentary organic matter. (45 hp)
461. Bokhari Friberg, Yasmin, 2015: The paleoceanography of Kattegat during the last deglaciation from benthic foraminiferal stable isotopes. (45 hp)
462. Lundberg, Frans, 2016: Cambrian stratigraphy and depositional dynamics based on the Tomten-1 drill core, Falbygden, Västergötland, Sweden. (45 hp)
463. Flindt, Anne-Cécile, 2016: A pre-LGM sandur deposit at Fiskarheden, NW Dalarna - sedimentology and glaciotectonic deformation. (45 hp)
464. Karlatou-Charalampopoulou, Artemis, 2016: Vegetation responses to Late Glacial climate shifts as reflected in a high resolution pollen record from Blekinge, south-eastern Sweden, compared with responses of other climate proxies. (45 hp)
465. Hajny, Casandra, 2016: Sedimentological study of the Jurassic and Cretaceous sequence in the Revinge-1 core, Scania. (45 hp)
466. Linders, Wictor, 2016: U-Pb geochronology and geochemistry of host rocks to the Bastnäs-type REE mineralization in the Riddarhyttan area, west central Berglsagen, Sweden. (45 hp)
467. Olsson, Andreas, 2016: Metamorphic record of monazite in aluminous migmatitic gneisses at Stensjöstrand, Sveconorwegian orogen. (45 hp)
468. Liesirova, Tina, 2016: Oxygen and its impact on nitrification rates in aquatic sediments. (15 hp)
469. Perneby Molin, Susanna, 2016: Embryologi och tidig ontogeni hos mesozoiska fisködlor (Ichthyopterygia). (15 hp)
470. Benavides Höglund, Nikolas, 2016: Digitization and interpretation of vintage 2D seismic reflection data from Hanö Bay, Sweden. (15 hp)
471. Malmgren, Johan, 2016: De mellankambriska oelandicuslagren på Öland - stratigrafi och faciestyper. (15 hp)
472. Fouskopoulos Larsson, Anna, 2016: XRF -studie av sedimentära borrkärnor - en metodikstudie av programvarorna Q-spec och Tray-sum. (15 hp)
473. Jansson, Robin, 2016: Är ERT och Tidsdomän IP potentiella karteringsverktyg inom miljögeologi? (15 hp)
474. Heger, Katja, 2016: Makrofossilanalys av sediment från det tidig-holocena undervattenslandskapet vid Haväng, östra Skåne. (15 hp)
475. Swierz, Pia, 2016: Utvärdering av vattenkemisk data från Borgholm kommun och dess relation till geologiska förhållanden och markanvändning. (15 hp)
476. Mårdh, Joakim, 2016: WalkTEM-undersökning vid Revingehed provpumpningsanläggning. (15 hp)
477. Rydberg, Elaine, 2016: Gummigranulat - En litteraturstudie över miljö- och hälsopåverkan vid användandet av gummigranulat. (15 hp)
478. Björnfors, Mark, 2016: Kusterosion och äldre kustdyners morfologi i Skälderviken. (15 hp)
479. Ringholm, Martin, 2016: Klimatutlöst matbrist i tidiga medeltida Europa, en jämförande studie mellan historiska dokument och paleoklimatarkiv. (15 hp)
480. Teilmann, Kim, 2016: Paleomagnetic dating of a mysterious lake record from the Kerguelen archipelago by matching to paleomagnetic field models. (15 hp)

LUNDS UNIVERSITET

Geologiska institutionen
Lunds universitet
Sölvegatan 12, 223 62 Lund